ACS OMEGA

Open Access

http://pubs.acs.org/journal/acsodf

Article

Chemical Degradation of Waste PET and Its Application in Wood Reinforcement and Modification

Tianle Xu, Zhibin Li, Xinran Ju, Hui Tang,* and Wenli Xiang

Cite This: *ACS Omega* 2023, 8, 30550−30562

Read Online

ACCESS | Metrics & More | Article Recommendations

ABSTRACT: In recent years, with the increasing scarcity of fossil resources and the worsening environmental pollution, the effective utilization of wood and plastic waste has become a critical issue. In this paper, propylene glycol (PG) was used as an alcoholysis agent to degrade waste poly(ethylene terephthalate) (PET), and unsaturated polyester (UPR) was synthesized by the polycondensation reaction. The Chinese fir was modified by chemical impregnation to obtain a new type of waste PET-based wood−plastic composites. It exhibits a compressive strength of about 107 MPa and a water absorption of less than 20%. These results highlight the outstanding modification effect on fir, demonstrating excellent mechanical properties and corrosion resistance. This study presents a green and efficient method for the preparation of wood−plastic composites and the recycling of waste PET, providing promising solutions for sustainable resource utilization and environmental protection.

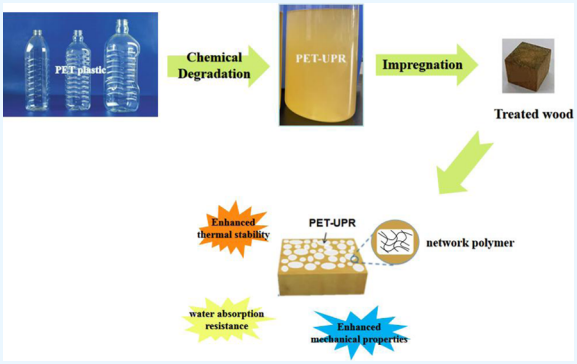

1. INTRODUCTION

Wood is a natural and renewable porous polymer material. As a green and environmentally friendly material, it has always been favored by people and is widely used in construction, industrial component construction, furniture production, indoor and outdoor decoration, and paper industries. However, due to the over-exploitation of natural forests in the past and the implementation of logging ban protection measures in recent years, the supply of high-quality wood is far from enough to meet the market demand.[1] Plantation trees not only have a short growth cycle but also have natural defects such as loose material, low mechanical strength, poor dimensional stability, easy mildew, and corrosion, which greatly limit their application range.[2,3]

PET is a high-performance engineering polymer with excellent mechanical and barrier properties; thus, it is used in large amounts nowadays, and it is widely used in plastic packaging bottles, films, and synthetic fibers.[4−6] Excellent comprehensive properties make PET the third most widely used polymer in the packaging industry, almost monopolizing the entire beverage packaging bottle market.[7] PET products such as plastic packaging bottles and polyester fibers have become an important part of living. The production of PET worldwide is also increasing year by year, and the annual output has increased from 42 million tons in 2014 to 74 million tons in 2020.[8−10] The design life of plastic is usually 1 to 50 years, but most plastic packaging materials lose their value after a short period of use.[11] Most plastics are difficult to decompose quickly in the ecosystem and easily accumulate in the environment after use, which causes serious environmental damage, known as "plastic pollution".[12]

In the chemical cyclic utilization process of PET, the polymer is depolymerized into oligomers or monomers, which are then separated, purified, and used as raw materials for the production of chemical products. Chemical recycling methods include hydrolysis, methanolysis, glycolysis, amine hydrolysis, ammonia hydrolysis, and other methods.[4,13] Hydrolysis is the only method that directly depolymerizes PET into TPA (terephthalic acid) and EG (ethylene glycol), and the reaction can be carried out in water media with different acid−base conditions. Since the technology for synthesizing PET directly from TPA and EG through esterification is well-established, and the production cost of TPA from para-xylene (PX) oxidation is relatively high, the recovery of TPA from waste PET materials through hydrolysis is of great significance. Hydrolysis can be classified into alkaline hydrolysis,[14] acid hydrolysis,[15] and neutral hydrolysis.[16] Based on the different alcoholysis agents, alcoholysis methods are generally divided into glycolysis[17] and methanolysis,[18] which are the two most commercially mature depolymerization methods. The amine

Received: May 30, 2023
Accepted: July 24, 2023
Published: August 8, 2023

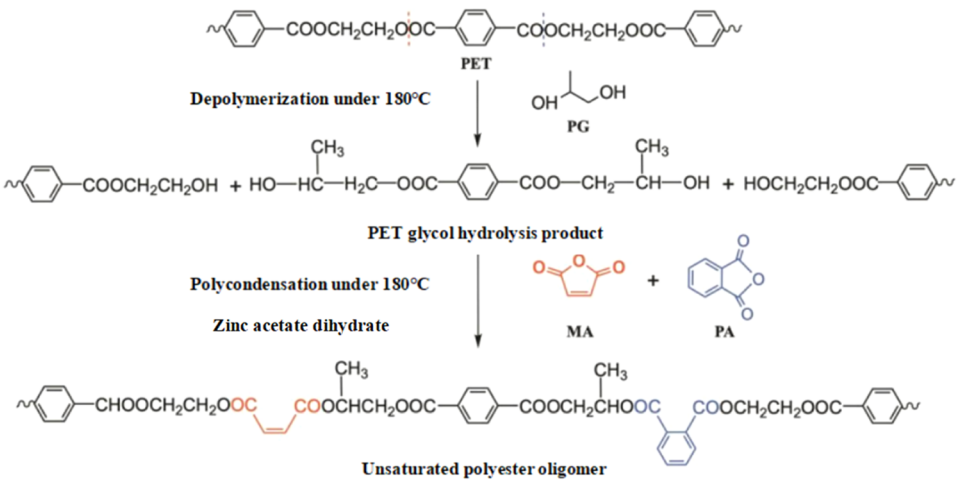

Figure 1. Schematic diagram of the reaction of PG alcoholysis of PET and the synthesis of UPR oligomers.

hydrolysis reaction of PET mainly produces TPA diamide and EG, and the most commonly used amine hydrolysis agents are methylamine, ethylamine, ethanolamine, and other primary amines, as well as ethylenediamine and other diamines, which are generally conducted within the temperature range of 20−100 °C.[16,19] In the related research of chemical recycling of waste PET, the main objectives are to improve the conversion rate and monomer yield of PET, shorten the reaction time, and conduct the reaction under milder conditions as much as possible. In recent years, numerous efforts have focused on the application of emerging technologies such as microwave heating,[20] supercritical fluids,[18,21] ionic liquids,[22−24] deep eutectic solvents,[25,26] etc. These approaches aim to address issues such as low thermal conductivity of PET, inadequate reaction contact, improvement of heat distribution in reactors, increase of depolymerization energy, enhancement of the effective contact area between PET and solvents/catalysts, and achievement of higher cyclic utilization efficiency.

Efficient cyclic utilization of discarded PET products to achieve renewable resource utilization is a major direction for the development of the green chemical industry. Duque-Ingunza et al.[27] catalyzed the ethanolysis of PET with Na_2CO_3, and the purified product was polycondensed with maleic anhydride to produce a linear unsaturated polyester. The resin was then cross-linked and cured using peroxide acetone and cobalt 2-ethylhexanoate, achieving the performance standards of commercial unsaturated polyester resins. However, the application of the polyester in some biomaterials has not been studied. Abdullah and Ahmad[28] synthesized UPR from ethanolysis of discarded PET and blended it with 0.3% coconut fibers to prepare coconut fiber-reinforced composite materials. In this study, the proportion of coconut fibers was relatively low, leaving room for further utilization of biomaterials. Wang et al.[29] reacted bifunctional epoxy oligomers with poly(ethylene glycol) to produce a waterborne epoxy resin, which was then impregnated into wood to study its related properties. For the impregnation modification of fir wood, Wang et al.[29] employed phenol−formaldehyde (PF) resin for chemical impregnation, while Liu et al.[30] used furfuryl alcohol (FA) resin for the modification of fir and poplar wood. However, the organic compounds used in these studies not only pose harm to human health but also do not adhere to the concept of green chemistry. To the best of our knowledge, there have been few studies on the application of UPR prepared from discarded PET in wood, achieving the combination of sustainable and green resource utilization, broadening the application range of fast-growing wood, and benefiting resource conservation and environmental protection.

We will establish a connection between wood and waste PET products, using propylene glycol as an alcoholysis agent and alcoholysis under high-temperature conditions; the PET ester bond is broken and replaced by hydroxyl end groups, and then, the addition of maleic anhydride (MA) and phthalic anhydride (PA) introduces double bonds and benzene rings into the molecular chain to obtain unsaturated polyester oligomers. The schematic diagram of the reaction is shown in Figure 1. Maleic anhydride provides active functional groups for the subsequent cross-linking of UPR oligomers; phthalic anhydride is used to adjust the double-bond content in the molecular chain of UPR oligomers, reduce the structural regularity, and increase the compatibility of UPR oligomers with cross-linking monomers while controlling its cross-linking density. Then, diluent styrene (St), cross-linking agent divinylbenzene (DVB), and initiator benzoyl peroxide (BPO) were added to the oligomer to prepare an impregnating liquid, which was modified by chemical impregnation.[31] The impregnation liquid was injected into the wood voids and cured. The result is a wood−plastic composite material with significantly improved mechanical properties, water absorption performance, and thermal stability. This further enhances the service life of the wood, improves its corrosion resistance and insect resistance, and provides a new solution for the recycling and utilization of waste PET plastics. It should be noted that the curing process of UPR is extremely complicated. The C═C bond on the linear unsaturated polyester molecular chain undergoes a free radical copolymerization reaction with styrene, which can form four possible cross-linking structures: (i) intermolecular cross-linking with or without the styrene monomer; (ii) intramolecular cross-linking with or without the styrene monomer; (iii) branching on polyester molecules by styrene; and (iv) a free styrene homopolymer.[32] Furthermore, the degree of polymerization of polystyrene between the cross-linked chains is different, and the existence of the steric hindrance effect also leads to some unreacted unsaturated double bonds in the cured product of the unsaturated polyester, which makes the resin-cured cross-linked network

https://doi.org/10.1021/acsomega.3c03805
ACS Omega 2023, 8, 30550−30562

highly chaotic and difficult to express clearly with chemical reaction formulas.

2. EXPERIMENTAL SECTION

2.1. Main Raw Materials and Instruments. *2.1.1. Experimental Materials and Reagents.* Industrial PET pellets, commercial 191-type resin (Purity: 99%), and Chinese fir were all purchased in the market. Waste PET recycled materials were obtained from PET bottle recycling and homemade. The alcoholysis agent 1,2-propanediol (PG, A.R. 99%) was purchased from Guangdong Guanghua Technology Co., Ltd., China. The catalyst zinc acetate dihydrate (A.R. 99%), the curing initiator benzoyl peroxide (BPO, A.R. 99%), the inhibitor hydroquinone (HQ, A.R. 99%), and dibutyl phthalate (A.R. 99%) were all provided by Sinopharm Group Chemical Reagent Co., Ltd., China. The diluent monomer styrene (St, A.R. 99%) and methyl methacrylate (MMA, A.R. 99%) were produced by Shanghai McLean Biochemical Science Co., Ltd., China. The cross-linking agent divinylbenzene (DVB, A.R. 80%) was purchased from Tianjin Baima Technology Co., Ltd., China. The drugs were used directly for the experiment without purification after purchase.

2.1.2. Analytical Testing Instruments. An NDJ-1 rotational viscometer (Shanghai Precision Scientific Instrument Co., Ltd.), a Fourier transform infrared spectrometer (FTIR, Spectrum Two, Perkin Elmer), a pressure testing machine (YAW-100D, Jinan Zhongluchang Testing Machine Manufacturing Co., Ltd.), a thermogravimetric analyzer (TGA, TGA-50, Shimadzu Corporation, Japan), an X-ray photoelectron spectrometer (XPS, PHI5000 Versaprobe-II, Ulvac-Phi, Japan), and a scanning electron microscope (SEM, Model TESCAN VEGA 3, Czech Tescan Company) were used.

2.2. PET Raw Material Processing. Industrial PET pellets were small elliptical cylinders (1.36 × 1.16 × 2.59 mm^3). Waste PET recycled materials were small square flakes (5 × 5 × 0.45 mm^3) cut from recycled PET packaging bottles. A 1% NaOH aqueous solution was used to soak the PET raw material for 1 h to remove surface impurities (oil stains), which was then washed with distilled water, dried in an oven at 80 °C for 2 h, and stored in a desiccator after treatment.

2.3. Preparation of Modified Wood Specimens. *2.3.1. Chemical Degradation of Waste PET and Synthesis of UPR.* In a three-necked flask, propylene glycol was added with a metering relationship of $n_{\text{propylene glycol}}/n_{\text{PET}}$ = 8:1, stirred, and heated up to 180 °C. Propylene glycol was taken as the benchmark, and 2 wt % zinc acetate dihydrate was added and reacted at a constant temperature for 9 h. The alcoholysis reaction was considered complete when all of the PET particles disappeared and the resulting product appeared transparent and clear in color. The alcoholysis products were used directly for the subsequent reaction without purification. When the temperature was reduced to 150 °C, the maleic anhydride (MA) and phthalic anhydride (PA) with the metering relationship of $n_{\text{alcoholysis system}}/n_{\text{acid anhydride}}$ = 1.2:1 (MA/PA = 1:1) were added. The device was changed to a reflux and distillation device. The stirring was started, and then it was heated up to 170−175°C, and the acid value was monitored according to GB/T 6743-2008.[33] When the acid value was decreased to about 135 mg KOH/g, the temperature was increased to 190−200°C to carry out the polycondensation reaction, until the acid value of the system decreased to 50 mg KOH/g. The heating was stopped, and 0.025 wt % hydroquinone was added to the total amount of the system when the temperature of the reaction system decreased to 120 °C. A preset ratio of the diluent/cross-linking agent was added when the temperature decreased to 90 °C; when the UPR oligomer was completely dissolved in the diluent/cross-linking agent, the stirring was stopped, and the waste PET-based UPR resin was prepared (Figure 2). The products were used for wood impregnation modification without undergoing purification.

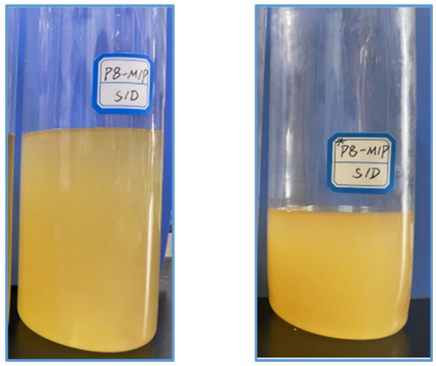

Figure 2. Industrial synthesis of PET-based UPR resin (left) and waste PET-based UPR resin (right).

2.3.2. Modification of Wood Specimens. In order to minimize the natural difference between the wood specimens (20 × 20 × 30 mm^3), the selected Chinese fir specimens should be sawn from the same board with a complete shape and no defects, and the density should be close to the average density. The Chinese fir specimens that were vacuum-dried at 103 ± 2 °C for 2 h were placed into the impregnation bottle and pre-evacuated for 30 min; then, under a pressure of −0.08 MPa, the UPR impregnation system with the preadded initiator was sucked into the impregnation bottle and submerged the wood specimen, and the vacuum impregnation at this pressure was maintained for 30 min. Finally, it was immersed under normal pressure for 2 h to ensure the complete immersion of the specimen,[34] and then the immersed wood samples were heated to solidify the immersion liquid inside the wood to complete the wood modification (Figure 3). Table 1 lists a summary of the experimental conditions of UPR-impregnated modified wood with Chinese fir as an example. In the experiment, to distinguish between industrial PET-based UPR-impregnated modified wood and waste PET-based UPR-impregnated modified wood, a "W" prefix was added to the waste PET-based UPR impregnation system.

2.4. Test Analysis Method. *2.4.1. FTIR Spectroscopy.* FTIR was used to characterize the structure of PET raw materials and PET alcoholysis products. The test resolution was 4 cm^{-1}, the number of scans was 32, and the test wavenumber range was 4000−400 cm^{-1}.

2.4.2. Determination of the Gel Content of the Dipping System. Determination of the gel content of the pure UPR resin impregnation system: according to the method in GB/T 2576-2005,[36] the soluble components in the UPR impregnation system after curing are extracted with ethyl acetate close to the boiling point temperature using a Soxhlet extractor, and the insoluble components are considered a cured resin. The gel content α is calculated according to formula 1

$$\alpha = \frac{m'}{m} \times 100\% \quad (1)$$

https://doi.org/10.1021/acsomega.3c03805
ACS Omega 2023, 8, 30550−30562

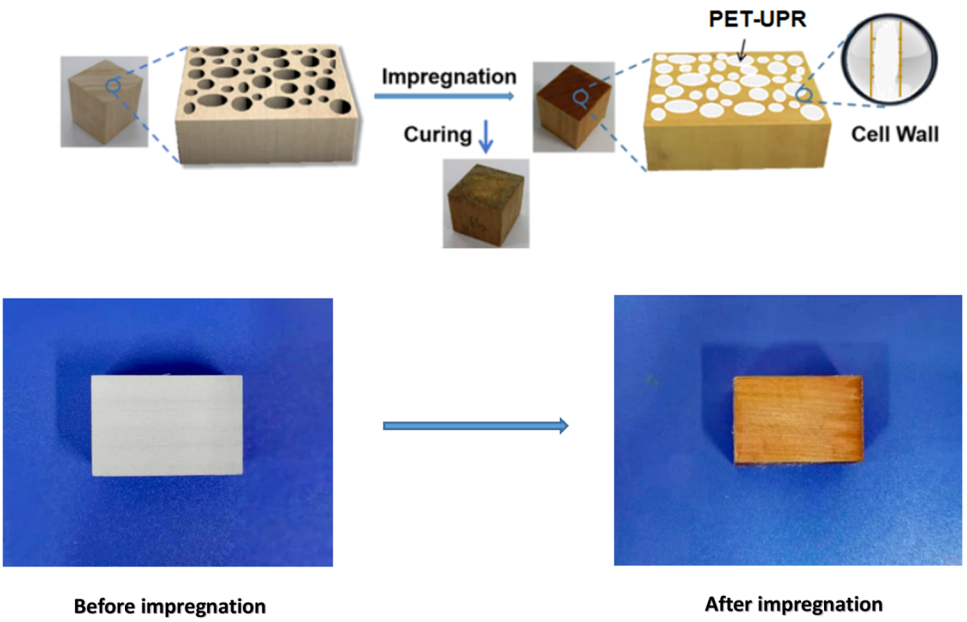

Figure 3. Schematic diagram of the impregnation and curing reaction of the PET-UPR system inside wood.[35]

Table 1. Combination of Experimental Conditions of UPR-Impregnated Modified Wood

modified wood code	wood species	UPR impregnation system	type of initiator	curing time (h)
W-S-P	S	P-S/D	BPO	6
S-191	S	191-UPR	BPO	6

where m is the mass of the sample before extraction, mg, and m' is the mass of the sample after extraction, mg.

Determination of the gel content of the UPR impregnation system in wood: with reference to the determination method of the gel content of the pure UPR impregnation system, the gel content β of the UPR impregnation system in wood is calculated according to formula 2

$$\beta = \frac{m_3 - m_2(1 - c_0)}{m_1 - m_2} \times 100\% \quad (2)$$

where m_1 is the mass of the modified wood sample before extraction, mg; m_2 is the mass of the log in the modified wood sample before extraction, mg; m_3 is the mass of the modified wood sample after extraction, mg; and c_0 is the log mass loss rate after extraction, %.

2.4.3. Determination of the Impregnation Rate and Curing Weight Gain Rate of Modified Wood. The impregnation rate IY of the UPR system impregnated wood is calculated according to formula 3, and the curing weight gain rate WPG is calculated according to formula 4

$$\mathrm{IY} = \frac{W_2 - W_1}{W_1} \times 100\% \quad (3)$$

$$\mathrm{WPG} = \frac{W_3 - W_1}{W_1} \times 100\% \quad (4)$$

where W_1 is the mass of the log specimen, g; W_2 is the mass of the wood specimen after impregnation, g; and W_3 is the mass of the wood specimen after curing, g.

2.4.4. Determination of the Water Absorption Resistance of Modified Wood. According to the measurement method in GB/T 1934.1-2009,[37] the measurement period was 8 days. The specimens were placed in an oven and subjected to a temperature of 60 °C for approx. 4 h. Subsequently, the drying and weighing procedures outlined in GB/T 1931-2009[38] sections 5.2 to 5.4 were followed. After the specimens were weighed, they were immediately placed into a container filled with distilled water. The specimens were submerged below the water surface by at least 50 mm using a stainless steel mesh and the container was securely covered. The water temperature was maintained within a range of (20 ± 2)°C. After 6 h, the specimens were weighed for the first time while still submerged in water. Subsequent weighings were conducted after 1, 2, 4, and 8 nights. The process continued until the difference in moisture content between the last two measurements was less than 5%, indicating that the maximum water absorption had been reached. The water absorption rate A of the modified wood specimen is calculated according to formula 5

$$A = \frac{m_n - m_0}{m_0} \times 100\% \quad (5)$$

In the formula, m_0 is the mass of the wood specimen when it is completely dry, g, and m_n is the mass of the wood specimen after water absorption, g.

The water absorption resistance WRE of the modified wood sample is calculated according to formula 6

$$\mathrm{WRE} = \frac{A_0 - A}{A_0} \times 100\% \quad (6)$$

In the formula, A_0 is the water absorption rate of the log specimen, %, and A is the water absorption rate of the modified wood specimen, %.

2.4.5. Determination of Compressive Strength along the Grain of Modified Wood. According to the method in GB/T 1935-2009,[39] a pressure testing machine is used to measure the compressive strength of wood specimens along the grain. The specimen is placed in the center of the spherical movable support of the testing machine along the grain direction, the loading speed is set to 0.5 KN/s, and the failure load of the specimen is recorded. The compressive strength along grain σ,

https://doi.org/10.1021/acsomega.3c03805
ACS Omega 2023, 8, 30550−30562

MPa, of the modified wood specimen is calculated according to formula 7

$$\sigma = \frac{P_{max}}{b \times t} \quad (7)$$

In the formula, P_{max} is the failure load, N; b is the width of the specimen, mm; and t is the length of the specimen, mm.

2.4.6. Thermogravimetric Analysis (TGA). The samples were processed with a pulverizer to a powder sample with a particle size of less than 0.2 mm, and the thermal stability of the modified wood was analyzed using TGA. The nitrogen flow was set to 20 mL/min, and the sample was heated from room temperature to 800 °C at a heating rate of 10 °C/min.

2.4.7. X-ray Photoelectron Spectroscopy (XPS). The log and modified wood specimens were cut from the chord direction into chord sections of 5 × 5 × 2 mm^3, and the surface chemical elements were analyzed by XPS. The Al anode was used as the X-ray source, the power was 50 KW, the pass energy was 46.95 eV, the step size of the XPS full spectrum and high-resolution spectrum were 0.8 and 0.2 eV, respectively, and the binding energy was C 1s of alkyl carbon (284.8 eV) for charge correction.

2.4.8. Scanning Electron Microscopy (SEM). The log and modified wood specimens were cut from the chord direction into chord section specimens of 5 × 5 × 2 mm^3, and the surface micromorphology was studied by SEM. The samples were sprayed with gold to avoid charge accumulation during characterization and then tested at 1000 and 5000 times magnification, separately, at an accelerating voltage of 20 KV.

3. RESULTS AND DISCUSSION

3.1. FTIR Analysis of PET Raw Materials and Products at Each Stage. Figure 4 shows the infrared spectra of industrial PET pellets, waste PET recycled materials, and their corresponding propylene glycol alcoholysis products and UPR oligomers from top to bottom. It can be seen that the characteristic absorption peaks of industrial PET pellets and waste PET recycled materials are completely consistent. The

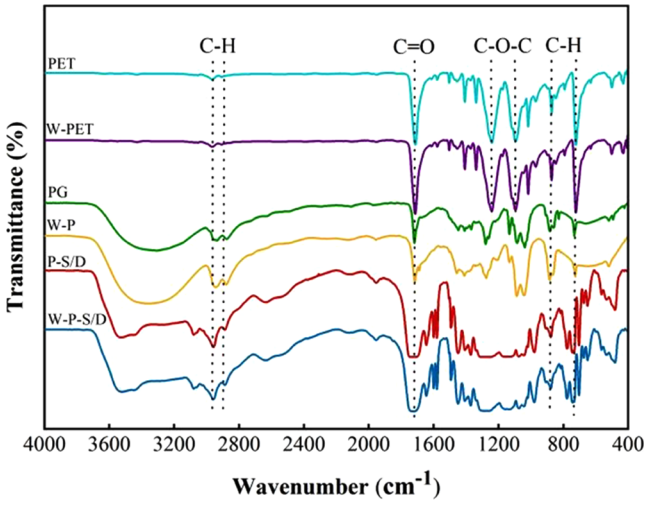

Figure 4. Infrared spectra of PET raw materials and corresponding products. In the figure, W-PET represents waste PET, W-P represents the alcoholysis products of waste PET, P-S/D represents the UPR oligomer synthesized from industrial PET, and W-P-S/D represents the UPR oligomer synthesized from waste PET.

double absorption peaks of C−H symmetric and antisymmetric stretching vibration near 2950 cm^{-1} indicate the existence of alkyl chains. 1720 cm^{-1} is the characteristic peak of the carbonyl group, and C−O−C symmetric and antisymmetric stretching vibration doublets appear at 1245 and 1110 cm^{-1}, respectively, indicating the existence of ester groups. The C−H stretching vibration of the para-disubstituted benzene ring appears near 880 and 730 cm^{-1}, indicating that there is a para-substituted benzene ring in the structure. The comparison results of characteristic peaks show that there is no difference in the chemical composition structure of industrial PET pellets and waste PET recycled materials, and they all completely accorded with the characteristic band properties of PET.

Figure 4 shows the C−H stretching vibration absorption peak of the alkyl group in the PET structure and the C═O stretching vibration absorption peak of the ester group. The C−H out-of-plane bending vibration absorption peaks of the para-disubstituted benzene ring appear at the same frequency position in the spectra of PET alcoholysis products and UPR oligomers, indicating that the PET glycolysis and UPR synthesis process successfully introduced some characteristic groups in the PET raw material structure into the subsequent stage products. In this experiment, UPR oligomers with a *p*-benzene structure were successfully synthesized. The introduction of unsaturated acid anhydrides and a reactive dilution system provided conditions for the cross-linking and curing of UPR.

3.2. Research on the UPR Impregnation System. *3.2.1. Analysis of Factors Influencing the Viscosity of the UPR Oligomer Mixture.* The viscosity of the UPR oligomer mixture to a certain extent reflects the impregnation ability of the resin system, directly impacting the performance of modified wood as a subsequent impregnation solution. In the synthesis process of UPR, both the dilution system and the PET raw material can affect the viscosity of the UPR oligomer mixture. This study referred to the curing method of commercial resin type 191 and selected styrene as the diluent[40] and DVB as the cross-linking agent. The selection of DVB was based on its unique double-bond structure, which allows for copolymerization with styrene, facilitating the introduction of functional groups while maintaining good strength. This has been widely applied in ion exchange resins.[41,42] The dilution system used in the UPR synthesis experimental scheme consisted of two active diluents, St and MMA, and one cross-linking agent, DVB, in the designed mass ratio of the UPR oligomer, as detailed in Table 2.

Table 2. Combination of Experimental Conditions for Determination of UPR Curing Reactivity

UPR oligomer mixture code	dilution system	type of initiator
P-S	30%St	BPO
P-S/D	30%St + 2%DVB	BPO
P-2S/M	20%St + 10%MMA	BPO

The viscosity of the UPR oligomer mixture is highest when solely using St as the dilution system, accounting for 30% of the total UPR oligomer content, as shown in Figure 5a. When an additional 2% of the cross-linking agent DVB is added to the dilution system, the viscosity of the UPR oligomer mixture noticeably decreases. Furthermore, when the dilution system consists of 20% St and 10% MMA, the viscosity of the UPR

https://doi.org/10.1021/acsomega.3c03805
ACS Omega 2023, 8, 30550−30562

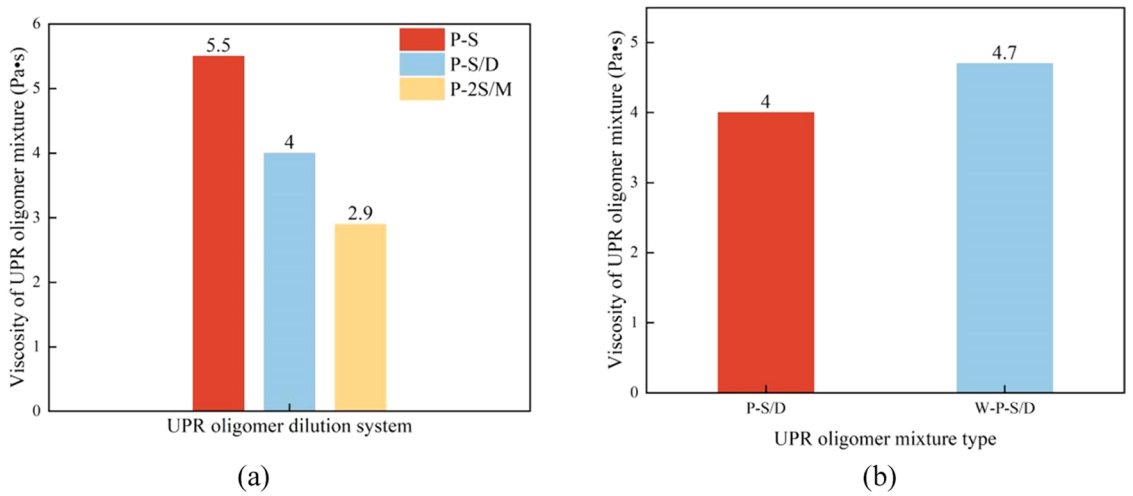

Figure 5. (a) Influence of dilution system on the viscosity of the UPR oligomer mixture. (b) Effect of the PET raw material on the viscosity of the UPR oligomer mixture.

oligomer mixture decreases significantly. From Figure 5b, it can be observed that the variation in PET raw materials has a relatively small impact on the viscosity of the UPR oligomer mixture. The UPR oligomer mixture synthesized from recycled PET waste through alcoholysis exhibits higher viscosity than industrial PET granules, which may be attributed to the use of recycled materials. The experimental substitution of MMA for a portion of styrene as a diluent in the comprehensive dilution conditions aims to investigate whether MMA can replace styrene as a new diluent. The results of this study will be discussed in the following sections.

3.2.2. Influence of the Dilution System on UPR Curing Reactivity. The curing reactivity of UPR was comprehensively evaluated by gel time, curing time, and exothermic peak temperature. The gel time and curing time are relatively short, and the curing reactivity of the UPR oligomer system with a higher exothermic peak temperature is relatively higher. In this experiment, St and MMA were used as active diluents for UPR oligomers, DVB was used as a cross-linking agent, and BPO was used as an initiator. The effect of the dilution system on the curing reactivity of UPR was investigated. Table 2 summarizes the combination of experimental conditions for the determination of UPR curing reactivity.

Table 3 lists the corresponding evaluation indicator data. When BPO is used as the initiator, the exothermic peak temperature of P-S/D is the highest, but its gel time and curing time are slightly longer than those for the other two systems (Figure 6). The addition of MMA as a diluent reduces the viscosity of the system, as shown in Figure 5a, but its performance in the curing reactivity experiment is not rational. The incorporation of the cross-linking agent DVB slightly extends the gel time and curing time, while it not only reduces the viscosity of the system (Figure 5a) but also increases the exothermic peak temperature. In a comprehensive comparison, the curing reactivity of P-S/D is better. Comprehensive analysis shows that the curing reactivity of P-S/D is better, and adding 2% of the bifunctional cross-linking agent DVB to the dilution system can significantly improve the curing reactivity of UPR.

Table 3. UPR Curing Reaction Activity Data of Dilution System

curing UPR	exothermic peak temperature (°C)	gel time(s)	curing time(s)
P-S	141.8	814	904
P-S/D	147.3	849	979
P-2S/M	112.0	781	892

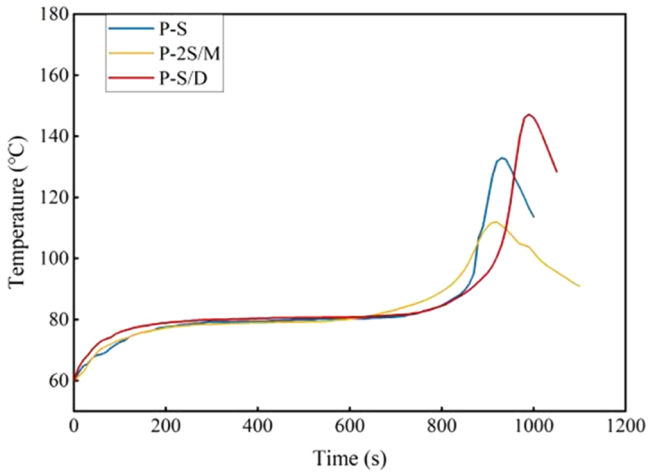

Figure 6. Comparison of the UPR curing activity of the PG dilution system. In the figure, P-S represents the complete dilution using styrene as the diluent, P-2S/M is the dilution with partial substitution of MMA for styrene, and P-S/D is the addition of the cross-linking agent DVB on the basis of styrene dilution. The specific amounts of additives are shown in Table 2.

3.2.3. Influence of PET Raw Materials on UPR Gel Content. According to the best plan of UPR curing, the UPR system synthesized from industrial PET pellets and waste PET recycled materials was cured at 80 °C for 3 h, showing degrees of cure of 86.5 and 81.8%, respectively. The reason for the slight decrease in the gel content of the UPR product may be the aging or oxidation of the recycled material due to light, heat, abrasion, and other factors during the use process. (Table 4) Even so, the gel content of UPR synthesized from PET recycled materials still reaches more than 80%, and it still has a high curing ability, which can be used for the research of impregnation and modification of fast-growing wood.

https://doi.org/10.1021/acsomega.3c03805
ACS Omega 2023, 8, 30550−30562

Table 4. Comparison of the Gel Content of UPR Synthesized from the PET Industrial Material and the Recycled Material[a]

cured UPR designation	curing temperature (°C)	curing time (h)	gel content (%)	standard deviation of gel content
P-S/D	80 ± 2	3	86.5	0.17
W-P-S/D	80 ± 2	3	81.8	0.25

[a]In the table, P-S/D represents industrial PET pellets and W-P-S/D represents waste PET recycled materials.

3.3. Properties of UPR-Impregnated Modified Wood.

3.3.1. Effect of the UPR Impregnation System on the Strengthening Properties of Modified Wood. Table 5 shows the impregnation rate, curing weight gain rate, and water absorption resistance data of different UPR impregnation systems in Chinese fir modification. It is found that the impregnation rate of PET-based UPR-impregnated modified fir is about 190%, the curing weight gain rate is 160−180%, and the water absorption resistance rate is 88−90%. In comparison, the waste PET-based UPR impregnation system and the industrial PET-based UPR impregnation system have significant effects on the impregnation weight gain and water absorption resistance of Chinese fir, which are almost the same. In the case of modified wood impregnated with 191-type commercially available UPR resin, it has been observed that the impregnation rate, curing weight gain rate, and water absorption resistance are marginally superior. Upon analysis, it has been deduced that the primary cause for this disparity lies in the substantially lower viscosity of the commercial UPR compared to the PET-based UPR system. Consequently, this results in relatively enhanced fluidity and wetting properties.

Figure 7 shows the water absorption and compressive strength curves of waste PET-based UPR-modified wood and logs. In Figure 7a, the water absorption of Chinese fir in 8 days is 167.3%, which is extremely unfavorable for the waterproof and anticorrosion requirements in the subsequent processing and application of wood. After impregnation and modification of waste PET-based UPR, the water absorption rate of Chinese fir in 8 days dropped to less than 20%, and the water absorption resistance of fast-growing wood was greatly improved. The compressive strength curves of Chinese fir before and after modification are shown in Figure 7b: the compressive strength of unmodified Chinese fir is 35.4 MPa, and the compressive strength of modified Chinese fir is 107.1 MPa, significantly improved.

3.3.2. Thermal Stability Analysis of UPR-Impregnated Wood. The thermogravimetric curve reflects the weight loss process of the sample as the temperature increases. Figure 8 shows the comparison of the thermogravimetric curves of the modified wood sample and the log sample, and the modified wood sample and the cured UPR sample.

It can be found from Figure 8 that the samples all have a relatively obvious weight loss process, and the weight loss process of the modified wood is slightly shifted to the high-temperature direction compared with the log. This weight loss process of curing UPR is slightly shifted toward higher temperatures compared to modified wood. The thermal decomposition of cured unsaturated polyester resin (W-P-S/D) can be explained through three main stages. The initial decomposition is observed before 250 °C, which is due to the evaporation of moisture and uncured materials on the surface of the resin, with a weight loss of around 8 wt %.[43,44] Subsequently, between 270 and 480 °C, a steep weight loss is exhibited, with the maximum DTG peak at approx. 394 °C. This is primarily due to the high temperature, causing rapid decomposition and volatilization of the cured UPR until the TGA and DTG curves return to their original baseline. Above 500 °C, a gradual and slow decrease in mass is observed, which is attributed to the slow oxidation of thermally stable carbon produced during the decomposition process.[45] According to the change of weight loss and weight loss rate of the sample with the change of temperature, the thermogravimetric analysis results of the log and modified wood are listed in Table 6.

It can be found from Table 6 that the weight loss change process of fir log and waste PET-based UPR-modified wood can be divided into four stages. The initial stage of weight loss from room temperature to 100 °C is mainly caused by the evaporation of residual moisture in the wood cell walls. The first stage is the dehydration stage. The weight loss rate of the modified wood at this stage is significantly lower than that of the log, which shows that under the same sample treatment conditions and storage environment, the modified wood can absorb less water with a lower saturation point, which refers to better water absorption resistance.

There is a large difference between the weight loss rate in the second stage. The quality of logs remains basically constant in the temperature range of 125−220 °C, which is a stage of slight weight loss. The weight loss rate of modified wood is 7.76% in the temperature range of 116−251 °C, mainly because a small part of the uncured UPR oligomers in the impregnation system have poor thermal stability, and weight loss occurs first.[46]

The third stage is the thermal decomposition stage, which is the main stage of log and modified wood weight loss. The weight loss rate of logs in the temperature range of 220−420 °C is 65.3%, mainly due to the pyrolysis of cellulose and hemicellulose.[47] The weight loss rate of modified wood is 74.49% in the temperature range of 251−456 °C, which is a mixed pyrolysis process of cellulose and hemicellulose of the wood itself and the UPR impregnation system after curing.

The fourth stage is the carbonization stage. The residual substances in the log and modified wood continue to be slowly pyrolyzed until carbonization, and the weight loss rate of the sample is low.

Comparing the thermal decomposition temperature range between the untreated spruce wood (S) and the waste PET-modified wood (W-S-P), it was observed that the thermal decomposition temperature of W-S-P was approx. 30 °C higher than that of S. This indicates that the modified wood

Table 5. Comparison of Properties of Modified Chinese Fir with Different UPR Impregnation Systems

UPR systems	wood type	viscosity (Pa·s)	P_{log} (g/cm^3)	P_{curing} (g/cm^3)	IY(%)	WPG (%)	WRE (%)
P-S/D	S	4.0	0.36	0.98	193.1	182.7	88.6
W-P-S/D	S	4.7	0.34	0.92	192.5	168.8	90
191-UPR	S	0.6	0.33	1.11	270.7	233.4	92.8

https://doi.org/10.1021/acsomega.3c03805
ACS Omega 2023, 8, 30550−30562

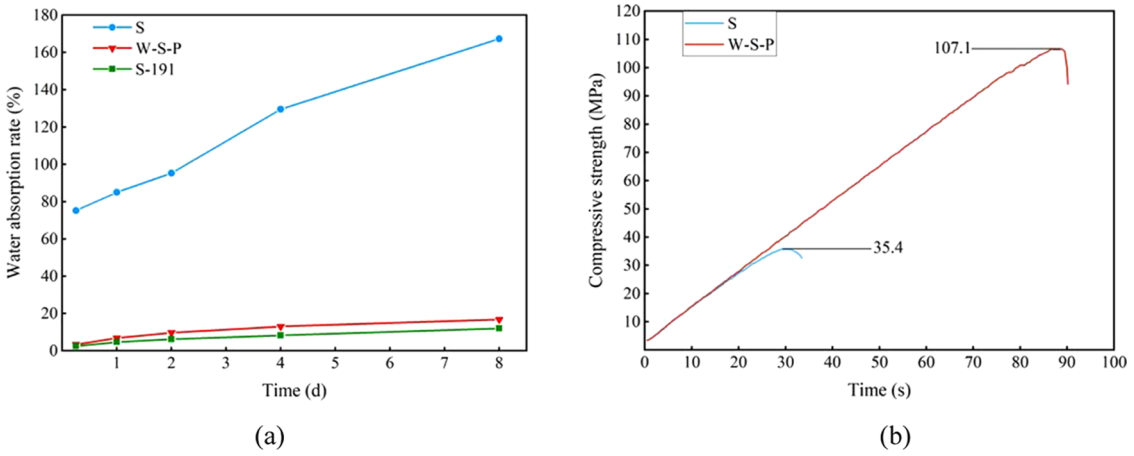

Figure 7. (a) Water absorption rate−time curves of modified woods and (b) compressive strength−time curves of modified woods. In the figure, S represents the unmodified spruce wood sample, and the codes and synthesis conditions for other wood−plastic composite materials can be found in Table 1.

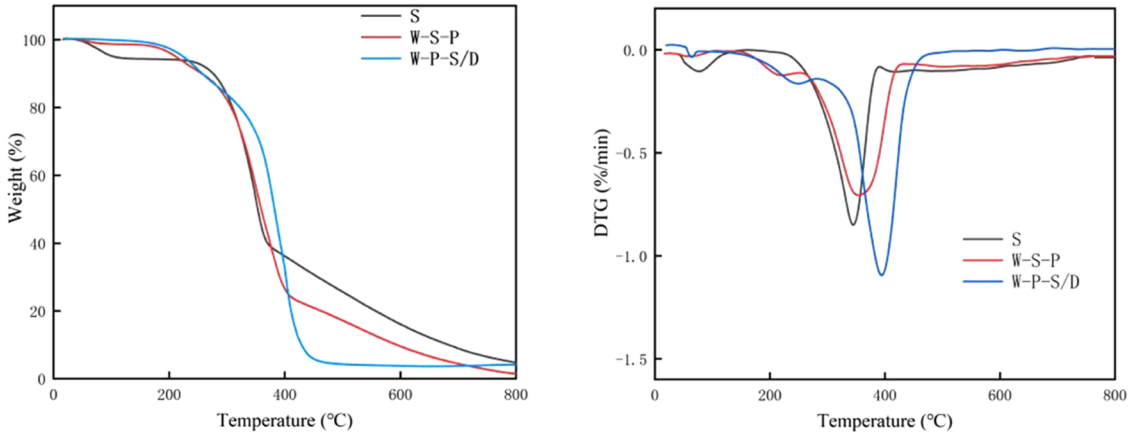

Figure 8. TGA and DTG curves of modified wood, cured UPR, and logs. In the figure, S represents the unmodified spruce wood, W-S-P refers to the wood−plastic composite material of modified spruce wood using W-P-S/D, and W-P-S/D represents the cured sample of waste PET-based unsaturated polyester resin.

Table 6. Thermogravimetric Analysis Results of Logs and Modified Woods

	stage 1		stage 2		stage 3		stage 4	
sample name	temperature range (°C)	weight loss rate	temperature range (°C)	weight loss rate (%)	temperature range (°C)	weight loss rate (%)	temperature range (°C)	weight loss rate (%)
S	21−125	4.14	125−220	0.5	220−420	65.31	420−800	10.16
W-S-P	21−116	1.22	116−251	7.76	251−456	74.49	456−800	4.99

exhibits relatively higher thermal stability. The thermogravimetric analysis further confirms that the impregnation modification of waste PET-based UPR resin has improved the thermal stability of fast-growing wood.

3.3.3. XPS Analysis of UPR-Impregnated Modified Wood. Chinese fir logs and Chinese fir-modified samples were selected for XPS characterization. Figures 9 and 10 are the XPS full scan spectrum and the C 1s high-resolution spectrum of each sample, respectively. It can be seen from the figure that the binding energy is 283−290 eV, and there are strong absorption peaks near 532 eV, indicating that the surface of Chinese fir logs and modified Chinese fir samples contains a large amount of C and O elements. The bonding state of C atoms in wood with other atoms or atomic groups can be divided into four forms.[48,49] In Figure 10, the C atoms of the C1 component correspond to aliphatic and aromatic carbon chains. C atoms are only combined with C or H atoms, mainly derived from lignin with the phenylpropane structure in logs, wood extracts, and the main chain structure in UPR. Its electron binding energy is about 284.8 eV.

The C2 component corresponds to the combination of C−O, and both cellulose and hemicellulose molecules in wood have a large number of C atoms connected to hydroxyl groups. Therefore, this combined state represents the chemical structural characteristics of cellulose and hemicellulose in wood. The electron binding energy is about 286.4 eV.

The C atom of the C3 component is related to the connection of two non-carbonyl-like O atoms or one carbonyl-like O atom, mainly derived from cellulose and hemicellulose.[50] The oxidation state of C is higher in the O−C−O structure. The electron binding energy is about 288 eV, which will give a significant chemical shift.

https://doi.org/10.1021/acsomega.3c03805
ACS Omega 2023, 8, 30550−30562

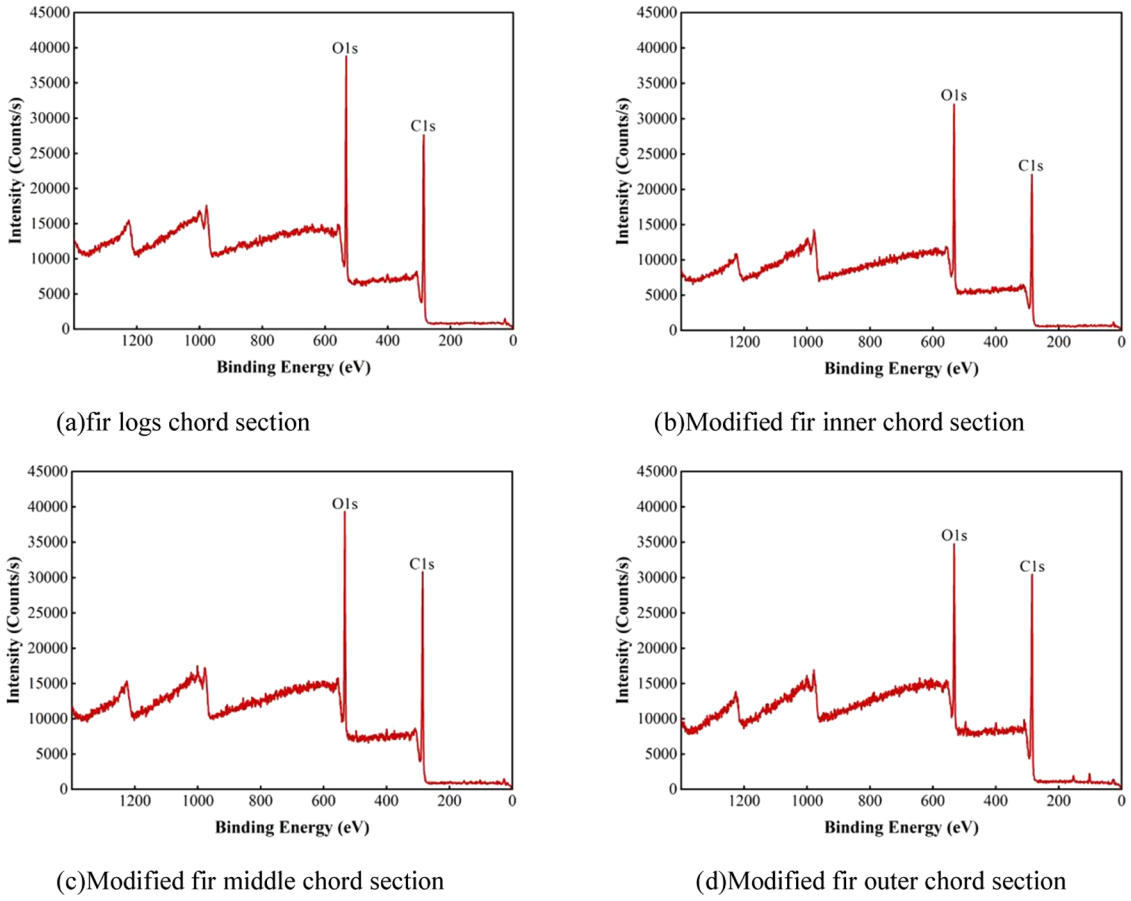

Figure 9. Survey XPS spectrum of Chinese fir log and waste PET-based UPR-impregnated modified Chinese fir samples.

The C atom of the C4 component is connected to a non-carbonyl-like O atom and a carbonyl-like O atom and has a high oxidation state with a binding energy of about 289 eV, which can produce a large chemical shift. Its main sources are fatty acids, acetic acid, and other substances in wood extracts and ester groups in unsaturated polyester resins.

In Table 7, from the chord section of the log sample to the inner, middle, and outer chord sections of the modified wood sample, the changes in the relative content of carbon atoms in different binding modes were observed. It can be seen that the carbon content ratio of C−C and O−C═O relative to the total carbon gradually increases, while the relative carbon content of C−O and O−C−O gradually decreases. At the same time, the total oxygen content and O/C of the samples showed a decreasing trend in the gradient direction from the log chord section to the inner, middle, and outer chord sections of the modified wood. The analysis showed that the relative content of cellulose and hemicellulose on the surface of modified Chinese fir decreased gradually from the inner chord section to the outer chord section compared with the fir log. After analysis, the reason for this changing trend is that the UPR with C−C and O−C═C as the characteristic link mode shows an increasing trend in this gradient direction. Moreover, the relative concentration of UPR on the outer chord section is slightly higher than that in the middle chord section, and that on the middle chord section is slightly higher than that in the inner chord section. The impregnation method of the resin is mainly transverse infiltration with a decreasing trend of permeability from outside to inside.

3.3.4. SEM Analysis of UPR-Impregnated Modified Wood. Figure 11 shows the scanning electron microscopy photos of the internal chord section samples of Chinese fir logs and modified Chinese fir W-S-P-B6. It can be seen from the figure that there are no obvious attachments in the duct molecules, wood fibers, and wood ray cells on the inner chord section of the log, and the pit openings and pit cavities are open, which provides a channel and place for the waste PET-based UPR system to penetrate into the cell cavity, intercellular space, pit, and other voids. In contrast, on the inner chord section of the modified wood, the vessel molecules, wood fibers, and wood ray cells were partially filled and adhered with translucent resin. The pit orifices were almost completely blocked by the resin, which indicates that the UPR system was successfully impregnated into the wood without destroying the microstructure of the wood.

The pits are the channels for water and other liquids to flow between the cells of the microscopic tissues of the wood. The UPR impregnation system blocks most of the pits in the wood, which reduces the permeability of the modified wood and greatly improves the water absorption resistance. Wood fibers (hardwood) and tracheids (softwood) in the wood structure play the main role of mechanical support. The UPR system fills, adheres to the cell walls of these cells, and further cross-links and solidifies, which in turn increases the compressive strength of the modified wood.

https://doi.org/10.1021/acsomega.3c03805
ACS Omega 2023, 8, 30550−30562

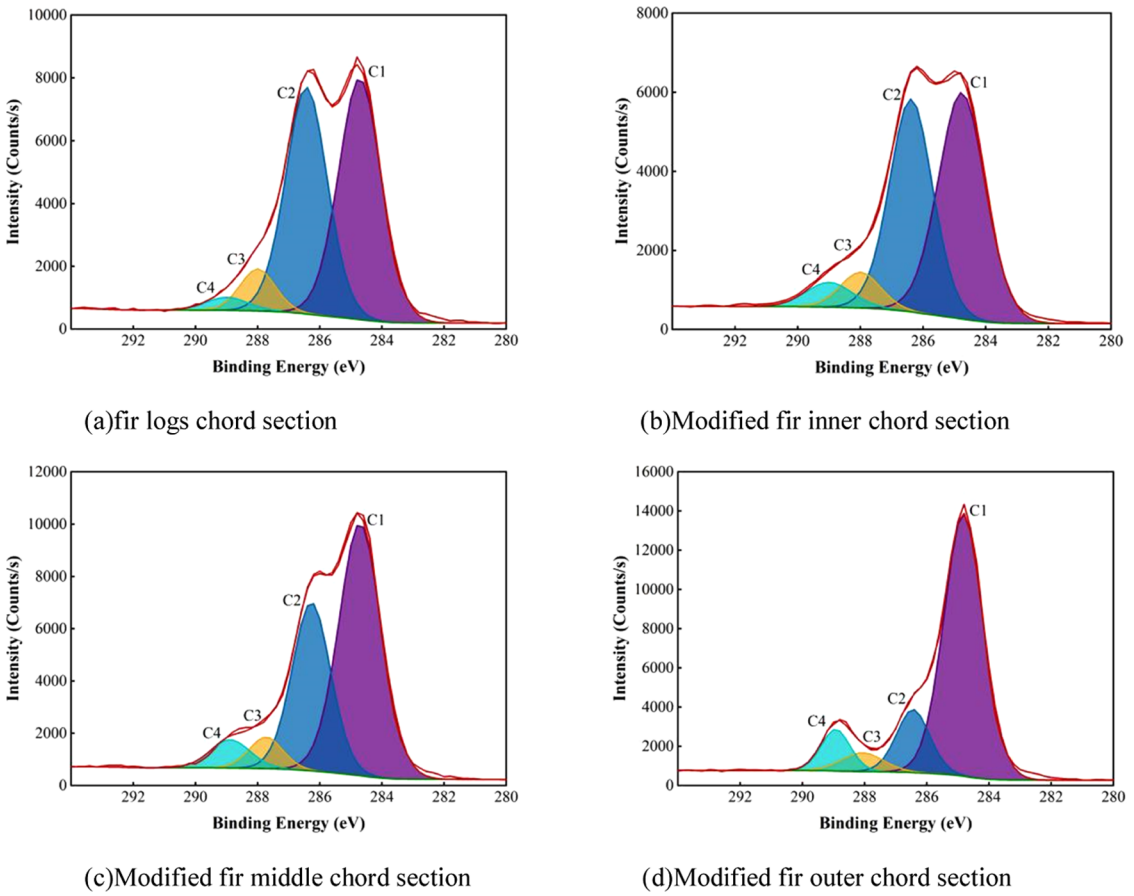

Figure 10. High-resolution C 1s XPS spectrum of Chinese fir log and waste PET-based UPR-impregnated modified Chinese fir samples.

Table 7. Contents of Chemical Elements on the Surface of Chinese Fir Log and Modified Chinese Fir Samples

sample serial number	C(%)	C−C(%)	C−O(%)	O−C−O(%)	O−C═O(%)	O(%)	O/C(%)
fir log chord section	68.86	32.49	29.92	4.71	1.74	29.37	42.65
modified fir inner chord section	67.61	32.09	27.67	4.37	3.48	30.65	45.33
modified fir middle chord section	69.20	38.09	23.24	3.83	4.04	28.64	41.39
modified fir outer chord section	71.38	50.93	10.44	3.96	6.05	24.40	34.18

4. CONCLUSIONS

In this paper, a *p*-benzene-type structure was introduced into the impregnation system by the method of depolymerizing waste PET with glycol. The chemical structure lays a foundation for the improvement of heat resistance, corrosion resistance, and mechanical properties of modified wood. The curing characteristics of PET-based UPR were comprehensively evaluated with gel time, curing time, exothermic peak temperature, and gel content as indicators to achieve the purpose of optimizing the UPR impregnation system and the wood modification process.

The FTIR analysis results of PET raw materials and products of each stage show that during the PET dihydric alcoholysis and UPR synthesis process, the characteristic groups such as alkyl groups, ester groups, and benzene ring para-position double substitution structures in the PET raw material structure were successfully added to the products of subsequent stages, and the UPR oligomer with the *p*-phenylene structure was successfully synthesized. The participation of unsaturated anhydride and the active diluent system provides the preconditions for the cross-linking and curing of UPR.

The XPS analysis results of waste PET-based UPR-impregnated modified wood stated that the relative content of UPR in the modified wood decreased gradually from the outer chord section to the inner chord section, which showed that the impregnation method of UPR is mainly transverse infiltration with a decreasing trend of permeability from outside to inside. It shows that the impregnation method of UPR is mainly transverse infiltration with a decreasing trend of permeability from outside to inside. The changes in the micromorphology observed by SEM indicated that the microstructure of the modified wood was not damaged. The UPR impregnation system fills and adheres to the vessel molecules, wood fibers, tracheids, wood rays, and other cells of the wood structural tissue and undergoes cross-linking and solidification. The pit openings on the cell wall are blocked, which greatly improves the water absorption resistance and mechanical strength of fast-growing wood. The results of thermogravimetric analysis show that the thermal decomposition initiation temperature of the waste PET-based UPR-impregnated modified wood is about 30 °C higher than that of the log and can maintain relatively high thermal stability.

https://doi.org/10.1021/acsomega.3c03805
ACS Omega 2023, 8, 30550−30562

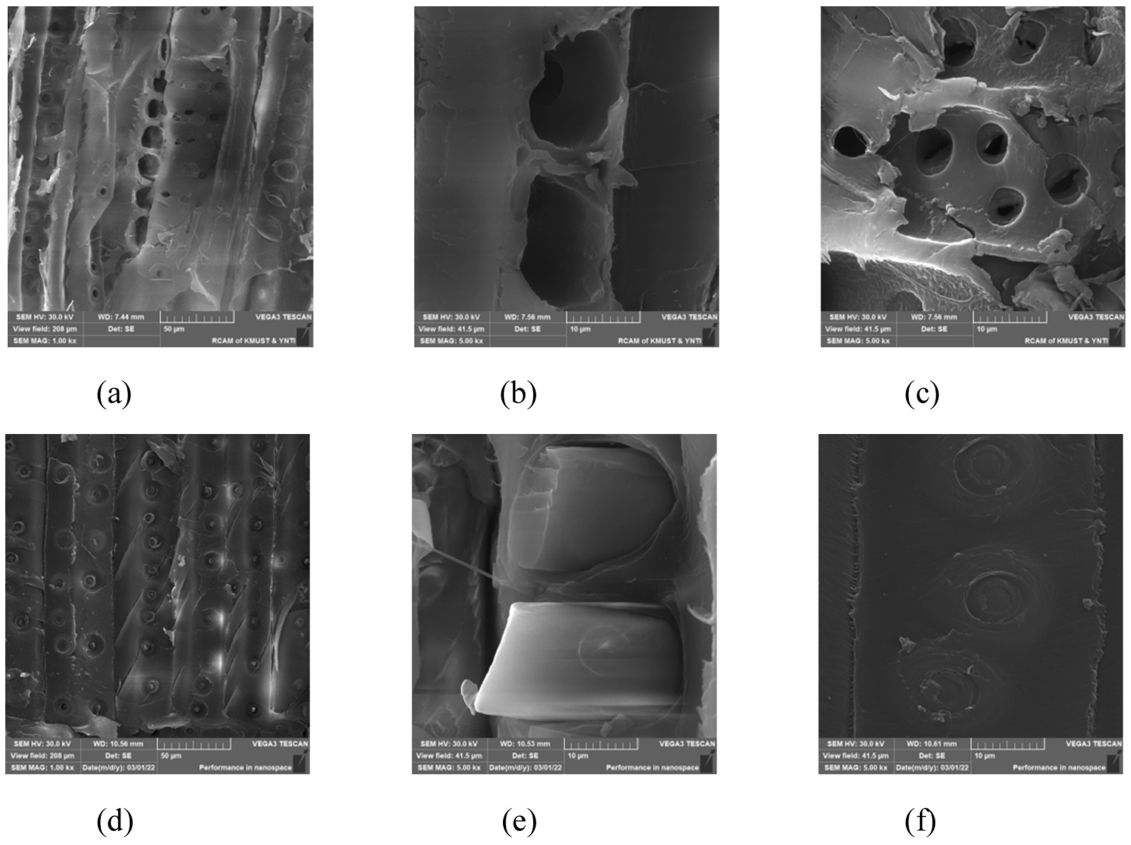

Figure 11. SEM pictures of Chinese fir log and waste PET-based UPR-impregnated modified Chinese fir samples. (a−c) SEM images of the internal chord section samples of Chinese fir logs. (d−f) SEM images of the modified Chinese fir internal chord section samples. (a) and (d) are 1000 times magnification, and (b), (c), (e), and (f) are 5000 times magnification.

This article solves the cyclic utilization of waste PET and the enhancement and modification of fast-growing wood. The modification effect is comparable to that of commercially available 191-type resin derived from fossil resources, which contains corrosion resistance, high mechanical strength, and thermal stability. This achievement embodies the scientific concept of green chemistry, aligning with the principles of sustainability and environmental responsibility in the realm of academic research.

AUTHOR INFORMATION

Corresponding Author

Hui Tang − *Faculty of Chemical Engineering, Kunming University of Science and Technology, Kunming 650032, China*; Email: thz9017@163.com

Authors

Tianle Xu − *Faculty of Chemical Engineering, Kunming University of Science and Technology, Kunming 650032, China*; orcid.org/0000-0003-3721-2659

Zhibin Li − *Faculty of Chemical Engineering, Kunming University of Science and Technology, Kunming 650032, China*

Xinran Ju − *Faculty of Science, University of Sydney, Camperdown 2050 New South Wales, Australia*

Wenli Xiang − *Faculty of Chemical Engineering, Kunming University of Science and Technology, Kunming 650032, China*

Complete contact information is available at: https://pubs.acs.org/10.1021/acsomega.3c03805

Notes

The authors declare no competing financial interest.

ACKNOWLEDGMENTS

I (T.X.) would like to express my gratitude to all of the individuals who had the privilege of working with me during this period and other related periods. Each member of my research team has provided me with abundant personal and professional guidance, imparting valuable knowledge about scientific research and life. Special thanks go to my graduate advisor, Professor Hui Tang. As my teacher and mentor, he not only provided me with valuable scientific guidance but also taught me how to find a balance between research and life. Additionally, I want to extend my appreciation to my family and friends for their immense encouragement and support throughout my journey. Their contributions and encouragement have been instrumental in my personal and academic growth, and I am truly grateful for their presence in my life.

REFERENCES

(1) Hoganson, H. M.; Meyer, N. G. Constrained Optimization for Addressing Forest-Wide Timber Production. *Curr. For. Rep.* **2015**, *1*, 33−43.

(2) Lang, Q.; et al. Cross-Linking Modifier Improves Applied Qualityof Fast-Growing Poplar. *Trans. Chin. Soc. Agric. Eng.* **2013**, *29*, 267−275.

(3) Tu, D. Research Progress of Thermo-Mechanical Compression Techniques for Wood Products. *J. For. Eng.* **2021**, *6*, 13−20.

(4) Ho, L. N. T.; Ngo, D. M.; Cho, J.; et al. Enhanced Catalytic Glycolysis Conditions for Chemical Recycling of Glycol-Modified Poly(Ethylene Terephthalate. *Polym. Degrad. Stab.* **2018**, *155*, 15−21.

(5) Veregue, F. R.; da Silva, C. T. P.; Moisés, M. P.; et al. Ultrasmall Cobalt Nanoparticles as a Catalyst for PET Glycolysis: A Green Protocol for Pure Hydroxyethyl Terephthalate Precipitation without Water. *ACS Sustainable Chem. Eng.* **2018**, *6*, 12017−12024.
(6) Niu, M.; Yang, Y.; Wang, X.; et al. Preparation and Characterization of Flame Retardant PET Fiber with Micro-encapsulated CMSs/PET. *J. Mater. Eng.* **2016**, *44*, 63−69.
(7) Nisticò, R. Polyethylene Terephthalate (PET) in the Packaging Industry. *Polym. Test.* **2020**, *90*, No. 106707.
(8) Bornscheuer, U. T. Feeding on Plastic. *Science* **2016**, *351*, 1154−1155.
(9) Cano, I.; Martin, C.; Fernandes, J. A.; et al. Paramagnetic Ionic Liquid-Coated SiO2@Fe3O4 Nanoparticles-the next Generation of Magnetically Recoverable Nanocatalysts Applied in the Glycolysis of PET. *Appl. Catal., B* **2020**, *260*, No. 118110.
(10) Tournier, V.; Topham, C. M.; Gilles, A.; et al. An Engineered PET Depolymerase to Break down and Recycle Plastic Bottles. *Nature* **2020**, *580*, 216−219.
(11) Gibb, B. C. "Plastics Are Forever. *Nat. Chem.* **2019**, *11*, 394−395.
(12) Taniguchi, I.; Yoshida, S.; Hiraga, K.; et al. Biodegradation of PET: Current Status and Application Aspects. *ACS Catal.* **2019**, *9*, 4089−4105.
(13) Geyer, B.; Lorenz, G.; Kandelbauer, A. Recycling of Poly(Ethylene Terephthalate) − a Review Focusing on Chemical Methods. *eXPRESS Polym. Lett.* **2016**, *10*, 559−586.
(14) Karayannidis, G. P.; Achilias, D. S. Chemical Recycling of Poly(Ethylene Terephthalate. *Macromol. Mater. Eng.* **2007**, *292*, 128−146.
(15) Ikenaga, K.; Inoue, T.; Kusakabe, K.; et al. Hydrolysis of PET by Combining Direct Microwave Heating with High Pressure. *Procedia Eng.* **2016**, *148*, 314−318.
(16) Al-Sabagh, A. M.; Yehia, F. Z.; Eshaq, G.; et al. Greener Routes for Recycling of Polyethylene Terephthalate. *Egypt. J. Pet.* **2016**, *25*, 53−64.
(17) George, N.; Kurian, T. Recent Developments in the Chemical Recycling of Postconsumer Poly(Ethylene Terephthalate) Waste. *Ind. Eng. Chem. Res.* **2014**, *53*, 14185−14198.
(18) Liu, Q.; Li, R.; Fang, T. Investigating and Modeling PET Methanolysis under Supercritical Conditions by Response Surface Methodology Approach. *Chem. Eng. J.* **2015**, *270*, 535−541.
(19) Malik, N.; Kumar, P.; Shrivastava, S.; et al. An Overview on PET Waste Recycling for Application in Packaging. *Int. J. Plast. Technol.* **2017**, *21*, 1−24.
(20) Mohsin, M. A.; Alnaqbi, M. A.; Busheer, R. M.; et al. Sodium Methoxide Catalyzed Depolymerization of Waste Polyethylene Terephthalate under Microwave Irradiation. *Catal. Ind.* **2018**, *10*, 41−48.
(21) dos Passos, J. S.; Glasius, M.; Biller, P. Screening of Common Synthetic Polymers for Depolymerization by Subcritical Hydrothermal Liquefaction. *Process Saf. Environ. Prot.* **2020**, *139*, 371−379.
(22) Yue, Q.; Xiao, L.; Zhang, M.; et al. The Glycolysis of Poly(Ethylene Terephthalate) Waste: Lewis Acidic Ionic Liquids as High Efficient Catalysts. *Polymers* **2013**, *5*, 1258−1271.
(23) Sun, J.; Liu, D.; Young, R. P.; et al. Solubilization and Upgrading of High Polyethylene Terephthalate Loadings in a Low-Costing Bifunctional Ionic Liquid. *ChemSusChem* **2018**, *11*, 781−792.
(24) Wang, L.; Nelson, G. A.; Toland, J.; et al. Glycolysis of PET Using 1,3-Dimethylimidazolium-2-Carboxylate as an Organocatalyst. *ACS Sustainable Chem. Eng.* **2020**, *8*, 13362−13368.
(25) Wang, Q.; Yao, X.; Geng, Y.; et al. Deep Eutectic Solvents as Highly Active Catalysts for the Fast and Mild Glycolysis of Poly(Ethylene Terephthalate)(PET). *Green Chem.* **2015**, *17*, 2473−2479.
(26) Liu, B.; Fu, W.; Lu, X.; et al. Lewis Acid−Base Synergistic Catalysis for Polyethylene Terephthalate Degradation by 1,3-Dimethylurea/Zn(OAc)2 Deep Eutectic Solvent. *ACS Sustainable Chem. Eng.* **2018**, *7*, 3292−3300.
(27) Duque-Ingunza, I.; López-Fonseca, R.; de Rivas, B.; et al. Synthesis of Unsaturated Polyester Resin from Glycolysed Post-consumer PET Wastes. *J. Mater. Cycles Waste Manage.* **2013**, *15*, 256−263.
(28) Abdullah, N. M.; Ahmad, I. Fire-Retardant Polyester Composites from Recycled Polyethylene Terephthalate (PET) Wastes Reinforced with Coconut Fibre. *Sains Malays.* **2013**, *42*, 811−818.
(29) Wang, J.; Yao, Y.; Huang, Y.; et al. Effects of the Combination of Compression and Impregnation with Phenolic Resin on the Dimensional Stability in the Multiscale Wood Structure of Chinese Fir. *Constr. Build. Mater.* **2022**, *327*, No. 126960.
(30) Liu, M.; Guo, F.; Wang, H.; et al. Highly Stable Wood Material with Low Resin Consumption via Vapor Phase Furfurylation in Cell Walls. *ACS Sustainable Chem. Eng.* **2020**, *8*, 13924−13933.
(31) Li, M.; et al. Research Status and Development Trend of Wood Functional Modification by Resin Impregnation. *China Wood-Based Panels* **2019**, *26*, 1−6.
(32) Gao, Y.; romero, P.; Zhang, H.; et al. Unsaturated Polyester Resin Concrete: A Review. *Constr. Build. Mater.* **2019**, *228*, No. 116709.
(33) CNOOC Changzhou Paint & Chemicals Research Institute. *Plastics (Polyester Resins) and Paints and Varnishes (Binders) -- Determination of Partial Acid Value and Total Acid Value. GB/T 6743-, Administration of Quality Supervision, Inspection and Quarantine of People's Republic of China; Standardization Administration of China*, 2008.
(34) Ma, Q.; Zhao, Z.; Yi, S.; et al. Modification of Fast-Growing Chinese Fir Wood with Unsaturated Polyester Resin: Impregnation Technology and Efficiency. *Results Phys* **2016**, *6*, 543−548.
(35) Ni, Z.; et al. Study on the Thermal Decomposition Kinetics of Unsaturated Polyester Resin. *Chem. Adhes.* **2021**, *43*, 1−4.
(36) China Building Materials Industry Association. *Test Method for Insoluble Matter Content of Resin Used in Fiber Reinforced Plastics. GB/T 2576-, General Administration of Quality Supervision, Inspection and Quarantine of the People Republic of China, China National Standardization Administration Committee*, 2005.
(37) Institute of Chinese Academy of Forestry Timber Industry. *Method for Determination of the Moistrure Content of Wood. GB/T 1931-, Administration of Quality Supervision, Inspection and Quarantine of People's Republic of China; Standardization Administration of China*, 2009.
(38) Institute of Chinese Academy of Forestry Timber Industry. *Method for Determination of the Moistrure Content of Wood. GB/T 1931-2009, Administration of Quality Supervision, Inspection and Quarantine of People's Republic of China; Standardization Administration of China*, 2009.
(39) *Method of Testing in Compressive Strength Parallel to Grain of Wood. GB/T 1935-, Administration of Quality Supervision, Inspection and Quarantine of People's Republic of China; Standardization Administration of China*, 2009.
(40) Jiang, L.; Zhu, J. A Study on Producing Putty with191-type of Unsaturated Polyester Resin *Hunan Chem. Ind.* 1998; Vol. *28* 5 DOI: 10.19342/j.cnki.issn.1009-9212.1998.05.008.
(41) Niu, G.; et al. Study on PVC-Poly (DMMA-divinyl benzene) Semi-homogeneous Cation Exchange Resin Mebrane. *Chem. Adhes.* **2006**, *28*, 443−445.
(42) He, B.; et al. Preparation and Characterization of Ion Exchange Resins (VI) - Porous High-Strength Resins. *At. Energy Sci. Technol.* **1964**, *7*, 515−522.
(43) Salasinska, K.; Celiński, M.; Barczewski, M.; et al. Fire Behavior of Flame Retarded Unsaturated Polyester Resin with High Nitrogen Content Additives. *Polym. Test.* **2020**, *84*, No. 106379.
(44) Kandola, B. K.; Ebdon, J. R. Flammability and Thermal Stability of Unsaturated Polyester Resin-Based Blends and Composites. *Unsaturated Polyester Resins* **2019**, 435−469.
(45) Halim, Z. A. A.; Yajid, M. A. M.; Nurhadi, F. A.; et al. Effect of Silica Aerogel − Aluminium Trihydroxide Hybrid Filler on the Physio-Mechanical and Thermal Decomposition Behaviour of

https://doi.org/10.1021/acsomega.3c03805
ACS Omega 2023, 8, 30550−30562

Unsaturated Polyester Resin Composite. *Polym. Degrad. Stab.* **2020**, *182*, No. 109377.
(46) Wang, D.; Ling, Q.; Nie, Y.; et al. In-Situ Cross-Linking of Waterborne Epoxy Resin inside Wood for Enhancing Its Dimensional Stability, Thermal Stability, and Decay Resistance. *ACS Appl. Polym. Mater.* **2021**, *3*, 6265−6273.
(47) Huai, C.; Fang, L.; et al. Thermogravimetric experiment and kinetic analysis of wood. *Fire Sci. Technol.* **2020**, *39*, No. 757.
(48) Nguila Inari, G.; Pétrissans, M.; Dumarcay, S.; et al. Limitation of XPS for Analysis of Wood Species Containing High Amounts of Lipophilic Extractives. *Wood Sci. Technol.* **2011**, *45*, 369−382.
(49) Hu, Y.; Hu, F.; Gan, M.; Xie, Y.; Feng, Q. A Rapid, Green Method for the Preparation of Cellulosic Self-Reinforcing Composites from Wood and Bamboo Pulp. *Ind. Crops Prod.* **2021**, *169*, No. 113658.
(50) Bañuls-Ciscar, J.; Pratelli, D.; Abel, M.-L.; Watts, J. F. Surface Characterisation of Pine Wood by XPS. *Surf. Interface Anal.* **2016**, *48*, 589−592.

https://doi.org/10.1021/acsomega.3c03805
ACS Omega 2023, 8, 30550−30562